Available online at www.sciencedirect.com
ScienceDirect
Journal of Hazardous Materials 147 (2007) 588–593
Journal of Hazardous Materials
www.elsevier.com/locate/jhazmat

Photocatalytic properties of nano-structured TiO_2-carbon films obtained by means of electrophoretic deposition

J.M. Peralta-Hernández [a], J. Manríquez [a], Y. Meas-Vong [a], Francisco J. Rodríguez [a], Thomas W. Chapman [a], Manuel I. Maldonado [b], Luis A. Godínez [a,*]

[a] *Electrochemistry Department, Centro de Investigación y Desarrollo Tecnológico en Electroquímica, Parque Tecnológico Querétaro Sanfandila, Pedro Escobedo, 76703 Querétaro, México*
[b] *Plataforma Solar de Almería-CIEMAT, Crta. Senés s/n, Tabernas, Almería 04200, Spain*

Received 12 October 2006; received in revised form 12 January 2007; accepted 15 January 2007
Available online 19 January 2007

Abstract

Recent studies have shown that the light-absorption and photocatalytic efficiencies of TiO_2 can be improved by coupling TiO_2 nano-particles with nonmetallic dopants, such as carbon. In this paper, we describe the electrophoretic preparation of a novel TiO_2-carbon nano-composite photocatalyst on a glass indium thin oxide (ITO) substrate. The objective is to take better advantage of the (e^-/h^+) pair generated by photoexcitation of semiconducting TiO_2 particles. The transfer of electrons (e^-) into adjacent carbon nano-particles promotes reduction of oxygen to produce hydrogen peroxide (H_2O_2) which, in the presence of iron ions, can subsequently form hydroxyl radicals ($^{\bullet}OH$) via the Fenton reaction. At the same time, $^{\bullet}OH$ is formed from water by the (h^+) holes in the TiO_2. Thus, the $^{\bullet}OH$ oxidant is produced by two routes. The efficiency of this photolytic-Fenton process was tested with a model organic compound, Orange-II (OG-II) azo dye, which is employed in the textile industry.

Keywords: Hydrogen peroxide; Nano-composite; Orange-II; Photocatalysis; Fenton

1. Introduction

Heterogeneous photocatalysis for water-treatment technologies has attracted the attention of many research groups around the world [1]. Among advanced oxidation processes (AOPs), photocatalytic treatment offers a capability for destroying organic contaminants by oxidation with hydroxyl radicals ($^{\bullet}OH$) that are generated under mild conditions [2,3]. The best-known photocatalyst is titanium dioxide (TiO_2). The band-gap value of anatase TiO_2 is around 3.2 eV, which enables UV light of wavelengths smaller than 400 nm to activate the catalyst [4]. The mechanism of photocatalysis involves the promotion of an electron (e^-) from the valence band (VB) into the conduction band (CB) of the semiconducting oxide, creating a hole (h^+) in the VB according to Eq. (1).

$$TiO_2 + h\nu \rightarrow e^-_{cb} + h^+_{vb} \quad (1)$$

In water, this process is followed by the formation of $^{\bullet}OH$ at the semiconductor surface as well as direct oxidation of organic compounds (R), according to the following reactions [5]:

$$h^+_{vb} + H_2O \rightarrow {}^{\bullet}OH + H^+ \quad (2)$$

$$h^+_{vb} + OH^- \rightarrow {}^{\bullet}OH_{ad} \quad (3)$$

$$h^+_{vb} + R_{ad} \rightarrow R^+ \quad (4)$$

Meanwhile, the electrons that are promoted to the CB can react with electron acceptors, such as oxygen, present in the solution [5]:

$$e^-_{cb} + O_2 \rightarrow O_2{}^{\bullet -} \quad (5)$$

In recent years, many studies have been made in order to improve the catalytic efficiency of TiO_2. The addition of other materials, for example carbon, has been of interest because this material can promote the adsorption of organic compounds to be transformed [6,7]. The effect of carbon on the photocatalytic efficiency of TiO_2 has been tested [8,9], and improved photocatalytic effectiveness has been reported by several authors

* Corresponding author. Tel.: +52 442 2116006; fax: +52 442 2116007.
E-mail address: lgodinez@cideteq.mx (L.A. Godínez).
URL: http://www.cideteq.mx (L.A. Godínez).

0304-3894/$ – see front matter © 2007 Elsevier B.V. All rights reserved.
doi:10.1016/j.jhazmat.2007.01.053

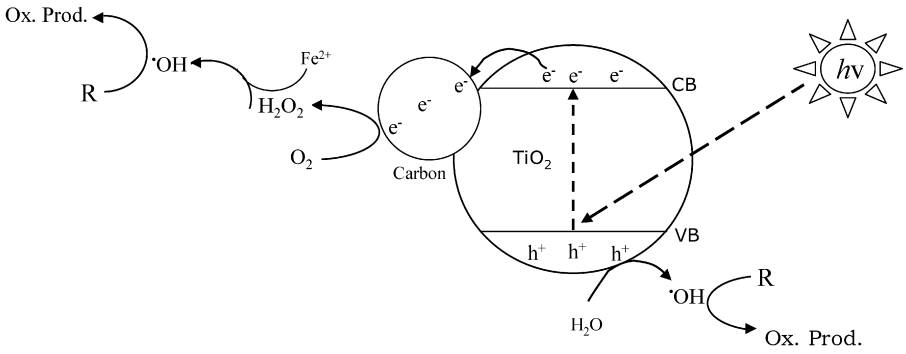

Fig. 1. Schematic diagram of the mechanism for the photocatalytic action of nano-structured TiO_2-carbon films on an organic target molecule. Direct oxidation occurs on the semiconductor, while electrons are transferred from the TiO_2 particles to the Vulcan carbon particle, forming peroxide by oxygen reduction, and promoting the Fenton reaction in solution.

[10–12]. Other workers have found that the recombination of holes and electrons, the major cause of inefficiency, can be retarded by applying a small positive potential to the TiO_2, and consequently the degradation of organic compounds through photoelectrocatalysis is enhanced [13]. According to research done by Egerton and Christensen [14], the method of preparation of the electrodes is the most important determinant factor for controlling the photocatalyst activity [15–17].

In this work, we report a preliminary study in which two approaches to water treatment are combined, photocatalysis and Fenton's reaction, which involves the homogeneous conversion of peroxide to $^{\bullet}OH$. Vulcan carbon has been incorporated with nanoscale TiO_2 particles in a mixed surface film, resulting in a nano-structured composite TiO_2-carbon photocatalyst for oxidative wastewater treatment. The overall reaction scheme is illustrated in Fig. 1. The electrons ejected by UV illumination to the CB can reduce dissolved oxygen (ORR) on the carbon surface to produce hydrogen peroxide. Ferrous ion in solution subsequently catalyzes the conversion of peroxide to $^{\bullet}OH$, an effective oxidant. At the same time $^{\bullet}OH$ is also produced directly from water by the holes in the semiconductor. With this scheme, we hope to enhance the degradation of organic compounds present in the water. In this study, the efficacy of the composite photocatalyst is tested by observing the decolorization of Orange-II (OG-II) azo dye as a model organic compound.

2. Materials and methods

2.1. Reagents and instruments

Nano-particulate TiO_2 (P25, 80% anatase, 20% rutile, average particle diameter 20 nm) was purchased from Degussa, and Vulcan carbon XC-72R (nominal average particle diameter 5 nm) was provided by CABOT. Conductive glass plates, TEC15, coated with SnO_2 films doped with indium (ITO), were supplied by Hartford Glass, USA. Analytical grade OG-II dye ($C_{16}H_{11}N_2NaO_4S$) was obtained from Aldrich, and used as received. Na_2SO_4, $FeSO_4{\cdot}7H_2O$, H_2SO_4, and 2-propanol 99.97% obtained from J.T. Baker were of analytical grade. Analytical grade oxygen (99.99%) was obtained from Infra. All solutions described in this work were prepared using water type I, according to ASTM-D1193-99$^{\varepsilon 1}$.

Cyclic voltammetry (CV) experiments were performed using a BAS-Zahner IM6 potentiostat/galvanostat in a three-electrode cell. Photocurrent spectroscopy (PS) experiments were made using a quartz cell irradiated with a Xe lamp 6257, 100 W, and a 77250 monochromator (Oriel); this arrangement was calibrated using an Eppley 17043 thermopile. Structural characterization of the films was carried out by X-ray diffraction (XRD) using a Bruker-AXS D8 Advanced diffractometer equipped with a Cu tube for generating Cu Kα radiation ($\lambda = 1.5406$ Å). Scanning electron microscopy (SEM) of the TiO_2 electrode surfaces was carried out using a JEOL-5400LV microscope.

The test for H_2O_2 production was conducted in 40 mL of a Na_2SO_4 solution (0.05 M) adjusted to pH 3 with H_2SO_4. The illumination was provided by a low-pressure mercury-vapor UV lamp (UVP Inc., $P = 75$ mW/cm^2, $\lambda = 365$ nm). The reactor was made of Duran® glass, and the illumination was direct. Hydrogen-peroxide concentration levels in the solution were determined by titration with titanium (IV) oxysulfate [$Ti(SO_4)_2$] with spectrophotometric detection at 406 nm [18]. Color changes in the course of the OG-II reaction were followed at $\lambda = 487$ nm, using a UV–vis spectrophotometer (Spectronic 20D$^+$ Milton Roy).

2.2. Electrophoretic deposition of nano-structured TiO_2-carbon films

Nano-composite electrodes were prepared by electrophoretic deposition (ED) of the particles on the ITO glasses plates immersed in 10 mL of a colloidal suspension (0.5 g P25 TiO_2 powder in 5% (v/v) 2-propanol). Various levels of carbon, ranging from 0 to 0.1 g, were used in the synthesis suspension, based on the method previously reported by Wahl and Augustynsky [19]. Accordingly, a 4 V potential difference was applied between a stainless-steel shield, and the negative ITO plate for a period of 40 s at room temperature. The distance between the electrodes was 2 cm. Following a previous report [20], fresh electrodes were placed in an oven to sinter the nano-composite film in air at 450 °C for 30 min, and they were then characterized by SEM, XRD, CV, and PS. They were then tested with respect to

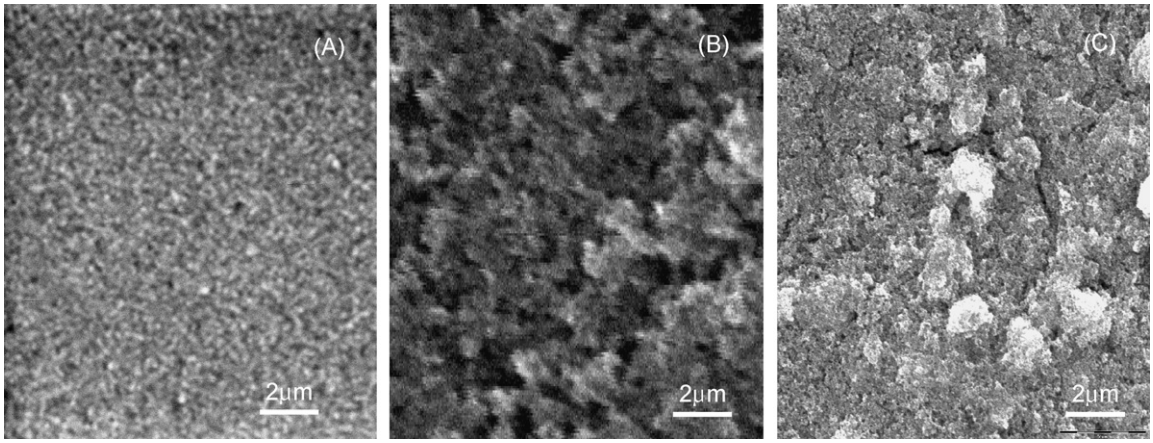

Fig. 2. SEM images of (A) ITO surface and films formed by ED, and subsequent sintering at 450 °C for 30 min; (B) TiO_2, and (C) nano-structured TiO_2-carbon films.

their photolytic activity for hydrogen-peroxide generation, and for their capacity to oxidize the test organic compound, OG-II. The supported films had a geometric surface of 0.16 cm^2, and a true area of 75 cm^2, as indicated by hydrogen adsorption in CV [21].

3. Results and discussion

3.1. Structure of the surface films

Representative SEM images of the experimental surfaces are shown in Fig. 2. Fig. 2A shows the fresh ITO surface. Figs. 2B and C present the films of TiO_2, and the composite TiO_2-carbon films, respectively, both prepared by ED with a deposition time of 40 s, and sintering. The difference between the simple TiO_2 film, and that containing carbon suggests the formation of aggregates that we ascribe to carbon particles in the TiO_2 film, and both are much rougher than the ITO substrate. Fig. 3 shows the structural characterization done by XRD measurements with a long time scan (10 s) and small steps (0.02° in 2θ). Fig. 3A shows a typical XRD spectrum of the pure nano-TiO_2 film, exhibiting 2θ diffraction angles between 20 and 50°. In this spectrum several principal peaks can be seen at 25.44, 37.92, and 48.16°, respectively; which can be assigned to diffraction

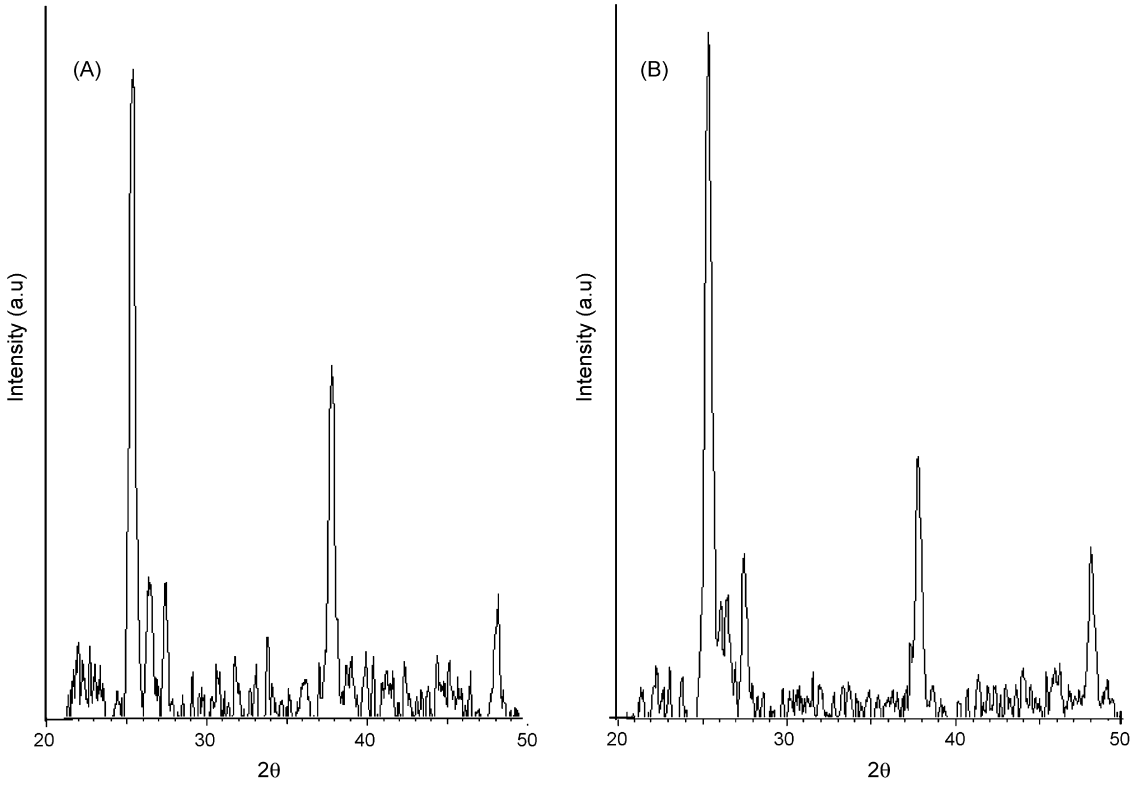

Fig. 3. XRD patterns of the electrodes deposited on ITO glass plates: (A) TiO_2 film without Vulcan carbon nano-particles, and (B) TiO_2-carbon film formed from a $0.005W_C$–$0.5W_{TiO_2}$ suspension.

from the (1 0 1), (0 0 4), and (2 0 0) planes of anatase, respectively [22]. Also, another peak appeared in 27.5° that can be associated with diffraction from the (1 1 0) plane of rutile. Thus, the film formed by ED of the TiO_2 particles retained mainly the anatase structure. Fig. 3B shows the comparable diffraction pattern for a sintered film formed from a suspension containing 0.005 g of C in the 10 mL suspension (denoted $W_c/W_{TiO_2} = 0.01$). It is seen that the pattern exhibits the same peaks (specially the principal diffraction peak at 25.44°, that corresponds to the anatase TiO_2 structure), but at the same time it is possible to discern the existence of a new signal around 26°, corresponding to the carbon present in the film [23]. With these assays, it is possible to infer that the carbon nano-particles present in the film do not introduce a significant change in the anatase structure.

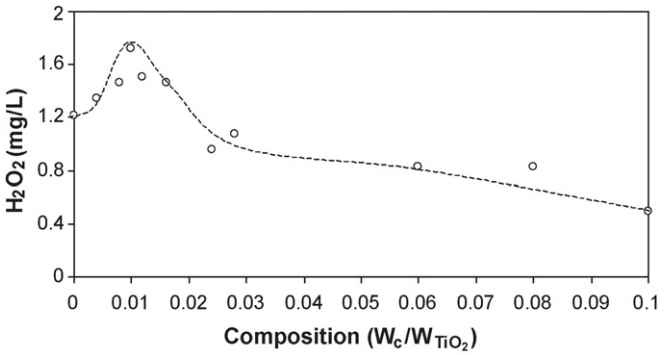

Fig. 4. Concentration of H_2O_2 produced after 60 min of photocatalytic reaction on the nano-structured TiO_2-carbon surface as a function of the carbon-TiO_2 ratio in the deposition suspension, pH 3. The UV light was supplied at $\lambda = 365$ nm, and $P = 75$ mW/cm^2.

3.2. Production of H_2O_2 from dissolved oxygen

The direct synthesis of hydrogen peroxide was tested by immersing the nano-scale TiO_2-carbon structures in 40 mL of an acidic solution (pH 3) containing dissolved oxygen, and illuminating directly the surfaces with UV light at $\lambda = 365$ nm. The radiant flux was estimated to be 75 mW/cm^2. The primary objective was to demonstrate the validity of the scheme postulated in Fig. 1, specifically the occurrence of the photolytic oxygen–reduction reaction (ORR) to produce H_2O_2, simultaneously with the reduction of water. The hydrogen peroxide concentration, attained after 60 min of illumination, was measured for films produced with various concentrations of carbon particles in the ED-synthesis suspension. The relevant results, presented in Fig. 4, show the peroxide concentration achieved after 60 min is a function of carbon level. It is seen that the H_2O_2 concentration produced with TiO_2 nano-particle films containing no carbon was only 1.2 mg/L, but when a low proportion of carbon nano-particles was present, the level of hydrogen peroxide increased by as much as 50%, achieving the value of 1.8 mg/L of H_2O_2. On the other hand, as the carbon level increased further, the peroxide concentration decreased, and fell below the pure-TiO_2 value. Presumably, this decrease results because an excess of carbon ultimately reduces the photocatalytic properties of the TiO_2 nano-particle. With too much carbon present, the light cannot penetrate adequately the TiO_2 lattice, and the photocatalytic charge separation is no longer possible. Based on Fig. 4, the best proportion of carbon in the ED process was $W_C/W_{TiO_2} = 0.01$. This condition was used for the subsequent tests.

3.3. Photocurrent spectroscopy and band-gap estimation

Action spectra for the TiO_2 films without carbon, and for TiO_2-carbon nano-structured films formed by ED ($W_C/W_{TiO_2} = 0.01$) at 40 s deposition time were determined in aqueous solution of $NaSO_4$ (0.05 M) adjusted to pH 3 with H_2SO_4. The incident-photon-to-current efficiency (IPCE) was calculated using the following relationship [24]:

$$\text{IPCE}(\%) = \frac{1240 \times j_{ph}}{\lambda \times \phi_0} \quad (6)$$

where j_{ph} corresponds to the photocurrent density (μA/cm^2), λ is the incident photon wavelength (nm), and ϕ_0 is the incident photon flux (W/m^2). The resulting IPCE versus λ curves are shown in Fig. 5A, where it is seen that the absorption region begins around 400 nm (that is, 3.0 eV, related to electron excitation of the Ti^{III}-H_2O doping sites) in close agreement with earlier reports [25–27]. Absorption by the carbon-bearing films is shifted to somewhat shorter wavelengths. In order to calculate

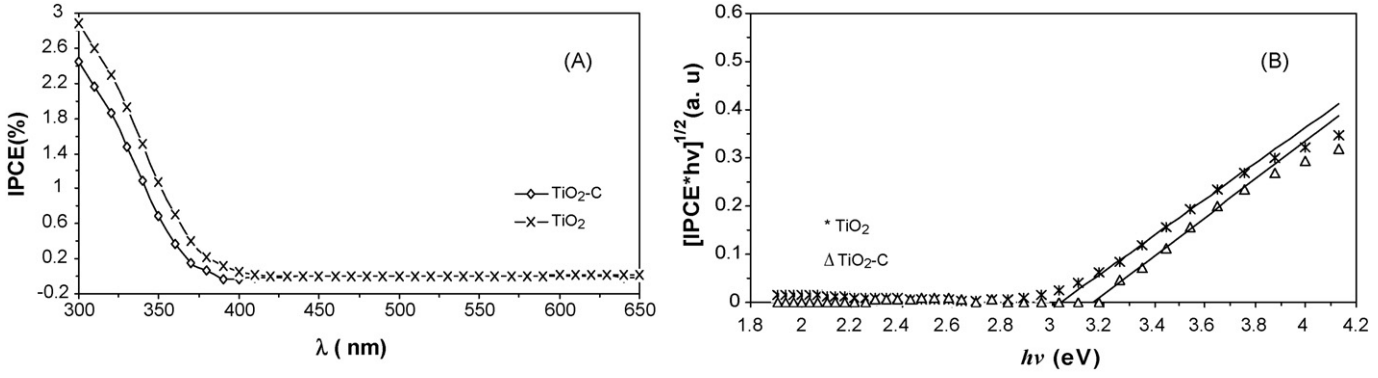

Fig. 5. Photovoltaic analysis of the semiconductor films: (A) Action spectra of nano-structured TiO_2 and TiO_2-carbon electrodes; (B) band-gap estimation for TiO_2, and nano-structured TiO_2-carbon electrodes, according to Eq. (7).

the band-gap energy values, ε_g, of the two films, we used the following relationship [28]:

$$(\text{IPCE} \times h\nu)^{1/2} \propto (h\nu - \varepsilon_g) \quad (7)$$

and plotted the data from Fig. 5A as $(\text{IPCE} \times h\nu)^{1/2}$ versus $h\nu$. The result is shown in Fig. 5B. According to the form of Eq. (7), the band-gap energies may be estimated from the X-axis intercepts to be 3.0 eV for the TiO_2 film, and 3.2 eV for the TiO_2-carbon. A possible explanation for this difference may be that the presence of the carbon in the sintered TiO_2 film affects the doping density of Ti^{III} within the nano-particulate semiconductor [27].

3.4. Electrochemical behavior of the compositeTiO2-carbon film on ITO

In order to evaluate the photoelectrocatalytic activity of the nano-structured TiO_2-carbon film, and to confirm its ability to promote the (ORR), we performed CV experiments in the dark, and under UV light irradiated at $\lambda = 365$ nm. The tests were conducted in an aqueous solution of $NaSO_4$ (0.05 M) adjusted to pH 3 with H_2SO_4 and saturated with pure oxygen (O_2) at atmospheric pressure. Measurements were taken between 0.547 V and −1.03 V versus SCE, and the scan rate was 50 mV/s. The results are shown in Fig. 6. For the simple TiO_2 film in the dark (Curve A), one observes essentially no signal with respect to the ORR on the film. With UV illumination, the TiO_2 film produced the response shown by Curve B. In this case, we see a cathodic peak at −0.7 V, which corresponds to the ORR on the TiO_2 film, with a current reaching about 6.2 mA/cm^2. Using the same conditions we tested the nano-composite material (TiO_2-carbon). In the dark, very little current was produced, as shown by Curve C. With UV illumination nano-composite TiO_2-carbon film produced the response shown as Curve D. In this case one sees a cathodic current rising to about 8.0 mA/cm^2, which is roughly 50% greater than that obtained with the TiO_2 alone. Thus, we may conclude that the composite material is an effective catalyst for the photolytic reduction of oxygen.

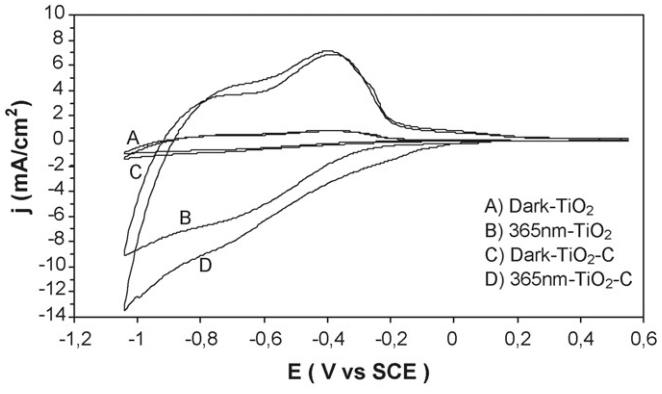

Fig. 6. Cyclic voltammograms for the TiO_2 and TiO_2-carbon electrodes, in aqueous Na_2SO4 (0.05 M) adjusted to pH 3 with H_2SO_4, and saturated with oxygen, in the dark, and under UV illumination at 365 nm.

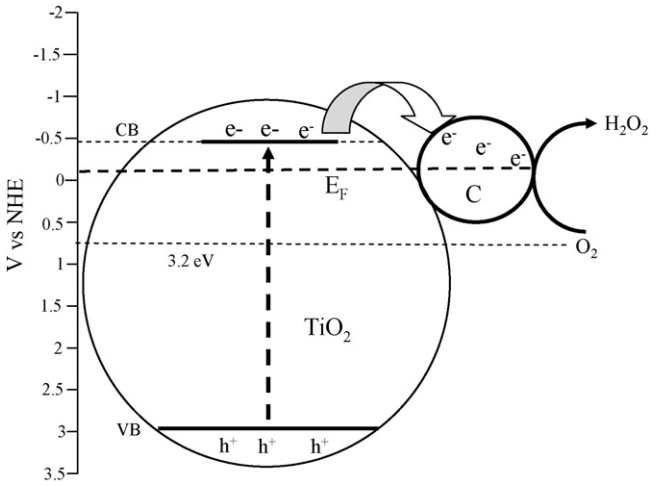

Fig. 7. Photochemical energetics of the TiO_2-carbon nano-structured film.

3.5. Interparticle electron transfer in the nano-structured TiO2-carbon film

Fig. 7 depicts the energetic relationships for the TiO_2-carbon material under UV light irradiation, with the photons being absorbed by the TiO_2 nano-particle thus yielding (e^-/h^+) pairs. The photogenerated electrons can be injected from the CB of TiO_2 to the Vulcan carbon particle because the level of the CB is −0.5 eV versus NHE, and the reduction potential of oxygen for the one-electron reduction is −0.2 eV versus NHE. Since this value is less negative than that of the CB potential of TiO_2, thermodynamic conditions favor the electron transfer from the semiconductor to the carbon particle.

3.6. Photocatalytic oxidation of a model organic compound

Fig. 1 suggests that the composite photocatalyst, when combined with ferrous ion in solution, should be able to oxidize species in solution by two simultaneous mechanisms: direct oxidation on the semiconductor by the photo-induced holes, and oxidation by $^{\bullet}OH$ formed from peroxide by the Fenton reaction. This premise was tested by comparing the rate of decol-

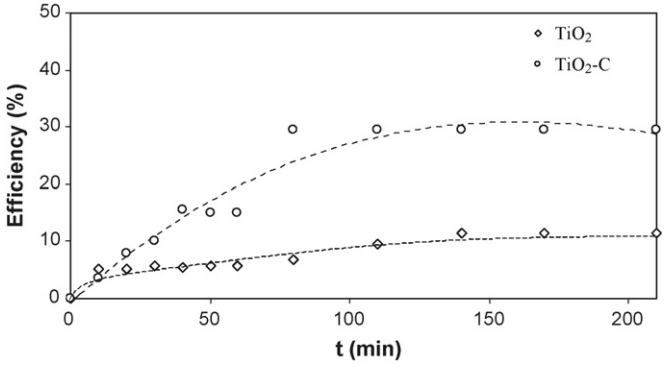

Fig. 8. Comparison of the fractional removal of color of a solution of aqueous OG-II dye (50 mg/L) versus time for films of TiO_2, and the composite TiO_2-carbon material, under UV illumination with addition of 0.01 mM of Fe^{2+}. The UV light was supplied at $\lambda = 365$ nm and $P = 75$ mW/cm^2.

orization of OG-II dye in solution (50 mg/L) when exposed to either a simple TiO_2 film or the composite TiO_2-carbon film, both exposed to UV light and in the presence of ferrous ion (0.01 mM). As shown in Fig. 8, one obtains with the composite catalyst about 30% removal of color within 2 h, which is more than three times the removal achieved with the simple TiO_2 photocatalyst.

4. Conclusions

This work presents a preliminary study of nano-structured, composite TiO_2-carbon photocatalysts. According to the results, it is possible to synthesize the composite films by ED. The resulting material was shown to promote photocatalytic oxygen–reduction, and our results indicate that, with an optimal ratio of carbon to TiO_2, it is possible to generate H_2O_2 in solution at a level 50% higher than that obtained by TiO_2, without carbon. With respect to the band-gap energies, the action spectra indicate that the value for the composite material formed with Vulcan carbon nano-particles is shifted by −0.2 eV, making possible interparticle electron transfer. Finally, it was shown that the TiO_2-carbon catalyst is more effective than simple TiO_2 for photolytic oxidation of an organic compound by combining the photocatalytic oxidation with Fenton's reaction.

Acknowledgments

The authors thank the Mexican Council for Science and Technology (CONACyT), and the Council for Science and Technology of Guanajuato (CONCyTEG) for financial support of this work (Grant GTO-04-C02-68). J.M.P.H also acknowledges CONACyT for a graduate fellowship. T.W.C. is a Cooperante supported by U.S. Peace Corps under agreement with CONACyT.

References

[1] P.R. Gogate, et al., A review of imperative technologies for wastewater treatment. I. Oxidation technologies at ambient conditions, Adv. Environ. Res. 8 (2004) 501–551.
[2] M.I. Franch, et al., Enhancement of photocatalytic activity of TiO_2 by adsorbed aluminium(III), Appl. Catal. B: Environ. 55 (2005) 105–113.
[3] D. Beydoun, et al., Role of nanoparticles in photocatalysis, J. Nanopart. Res. 1 (1999) 439–458.
[4] A.H.C. Chan, et al., Solar photocatalytic thin film cascade reactor for treatment of benzoic acid containing wastewater, Water Res. 37 (2003) 1125–1135.
[5] J.M. Peralta-Hernández, et al., In situ electrochemical and photoelectrochemical generation of the fenton regent, a potentially important new water treatment, Water Res. 40 (2006) 1754–1762.
[6] G. Colón, et al., A novel preparation of high surface area TiO_2 nanoparticles from alkoxide precursor and using active carbon as additive, Catal. Today 76 (2002) 91–1001.
[7] G. Colón, et al., Influence of residual carbon on the photocatalytic activity of TiO_2/C samples for phenol oxidation, Appl. Catal. B: Environ. 43 (2003) 163–173.
[8] B. Tryba, et al., Application of TiO_2-mounted activated carbon to the removal of phenol from water, Appl. Catal. B: Environ. 41 (2003) 427–433.
[9] B. Tryba, et al., Hybridization of adsorptivity with photocatalytic activity-carbon-coated anatase, J. Photochem. Photobiol. A: Chem. 167 (2004) 127–135.
[10] M. Janus, et al., New preparation of a carbon-TiO_2 photocatalysis by carbonization of *n*-hexane deposited on TiO_2, Appl. Catal. B: Environ. 52 (2004) 61–67.
[11] J. Matos, et al., Synergy effect in the photocatalytic degradation of phenol on a suspended mixture of titania and activated carbon, Appl. Catal. B: Environ. 18 (1998) 281–291.
[12] J.M. Herrmann, et al., Solar photocatalytic degradation of 4-chlorophenol using the synergistic effect between titania and activated carbon in aqueous suspension, Catal. Today 54 (1999) 255–265.
[13] T.A. Egerton, et al., New TiO_2/C sol–gel electrodes for photoelectrocatalytic degradation of sodium oxalate, Chemosphere 63 (2006) 1203–1208.
[14] T.A. Egerton, P.A. Chritensen, Photoelectrocatalysis processes, in: S. Parsons (Ed.), Advanced Oxidation Processes for Water and Wastewater Treatment, IWA Publishing, London, UK, 2004, pp. 167–184.
[15] H. Hidaka, et al., A mechanistic study of the photoelectrochemical oxidation of organic compounds on a TiO_2/TCO particulate film electrode assembly, J. Photochem. Photobiol. A: Chem. 98 (1996) 73–78.
[16] J.A. Byrne, et al., Photochemistry of oxalate on particulate TiO_2 electrodes, J. Electroanal. Chem. 457 (1998) 675–677.
[17] C. He, et al., The enhanced PC and PEC oxidation of formic acid in aqueous solution using a Cu-TiO_2/ITO film, Chemosphere 58 (2005) 381–389.
[18] G.M. Eisenberg, Colorimetric determination of hydrogen peroxide, Ind. Eng. Chem. 15 (1943) 327–328.
[19] A. Wahl, J. Augustinsky, Charge carrier transport in nanostructured anatase TiO_2 films assisted by the self-doping of nanoparticles, J. Phys. Chem. B 102 (1998) 7820–7828.
[20] B. O'Regan, M. Grätzel, A low-cost, high-efficiency solar cell based on dye-sensitized colloidal TiO_2 films, Nature 353 (1991) 737–740.
[21] H. Pelouchova, et al., Charge transfer reductive doping of single crystal TiO_2 anatase, J. Electroanal. Chem. 566 (2004) 73–83.
[22] L. Yangming, et al., Preparation and application of nano-TiO_2 catalyst in dye electrochemical treatment, Water SA 32 (2006) 205–209.
[23] N. Keller, et al., Macroscopic carbon nanofibers for use as photocatalyst support, Catal. Today 101 (2005) 323–329.
[24] C.A. Bignozzi, et al., Molecular and supramolecular sensitization of nanocrystalline wide band-gap semiconductors with mononuclear and polynuclear metal complexes, Chem. Soc. Rev. 29 (2000) 87–96.
[25] H. Kozuka, et al., Preparation and photoelectrochemical properties of porous thin films composed of submicron TiO_2 particles, Thin Solid Films 358 (2000) 172–179.
[26] F. Cao, et al., Electrical and optical properties of porous nanocrystalline TiO_2 films, J. Phys. Chem. B 99 (1995) 11974–11980.
[27] J. Manríquez, L.A. Godínez, Tuning the structural, electrical and optical properties of Ti(III)-doped nanocrystalline TiO_2 films by electrophoretic deposition time, Thin Solid Films 515 (2007) 3402–3413.
[28] J.D. Kim, et al., Effect of hydrogen on stresses in anodic oxide film on titanium, Electrochim. Acta 48 (2003) 1123–1130.